

ISSN: (Print) (Online) Journal homepage: <https://www.tandfonline.com/loi/tbsd20>

Identifying inhibitors of NSP16-NSP10 of SARS-CoV-2 from large databases

Hoang Linh Nguyen, Nguyen Quoc Thai & Mai Suan Li

To cite this article: Hoang Linh Nguyen, Nguyen Quoc Thai & Mai Suan Li (2022): Identifying inhibitors of NSP16-NSP10 of SARS-CoV-2 from large databases, Journal of Biomolecular Structure and Dynamics, DOI: [10.1080/07391102.2022.2114941](https://doi.org/10.1080/07391102.2022.2114941)

To link to this article: <https://doi.org/10.1080/07391102.2022.2114941>



View supplementary material [↗](#)



Published online: 24 Aug 2022.



Submit your article to this journal [↗](#)



Article views: 15



View related articles [↗](#)



View Crossmark data [↗](#)



Identifying inhibitors of NSP16-NSP10 of SARS-CoV-2 from large databases

Hoang Linh Nguyen^{a,b,c,*}, Nguyen Quoc Thai^{d,*} and Mai Suan Li^e 

^aLife Science Lab, Institute for Computational Science and Technology, Quang Trung, Software City, Ho Chi Minh City, Vietnam; ^bHo Chi Minh City University of Technology (HCMUT), Ho Chi Minh City, Vietnam; ^cVietnam National University, Ho Chi Minh City, Vietnam; ^dDong Thap University, Cao Lanh City, Dong Thap, Vietnam; ^eInstitute of Physics, Polish Academy of Sciences, Warsaw, Poland

Communicated by Ramaswamy H. Sarma

ABSTRACT

The COVID-19 pandemic, which has already claimed millions of lives, continues to pose a serious threat to human health, requiring the development of new effective drugs. Non-structural proteins of SARS-CoV-2 play an important role in viral replication and infection. Among them, NSP16 (non-structured protein 16) and its cofactor NSP10 (non-structured protein 10) perform C2'-O methylation at the 5' end of the viral RNA, which promotes efficient virus replication. Therefore, the NSP16-NSP10 complex becomes an attractive target for drug development. Using a multi-step virtual screening protocol which includes Lipinski's rule, docking, steered molecular dynamics and umbrella sampling, we searched for potential inhibitors from the PubChem and anti-HIV databases. It has been shown that CID 135566620 compound from PubChem is the best candidate with an inhibition constant in the sub- μ M range. The Van der Waals interaction was found to be more important than the electrostatic interaction in the binding affinity of this compound to NSP16-NSP10. Further *in vitro* and *in vivo* studies are needed to test the activity of the identified compound against COVID-19.

ARTICLE HISTORY

Received 11 May 2022
Accepted 14 August 2022

KEY WORDS

Virtual screening; SARS-CoV; COVID-19; SARS-CoV-2 (nCoV); umbrella sampling; NSP16-NSP10; COVID-19

1. Introduction

Over the past two decades, betacoronaviruses have triggered two epidemics, namely the severe acute respiratory syndrome coronavirus (SARS-CoV) and the Middle East respiratory syndrome coronavirus (MERS-CoV) (Skowronski et al., 2005). In 2019, an outbreak of a new coronavirus in Wuhan, China, turned into a global pandemic called COVID-19 (World Health Organization, 2020), which has claimed more than 5.2 million lives worldwide. Based on genetic analysis, this new virus has been named SARS-CoV-2 due to its close relationship with SARS-CoV (Coronaviridae Study Group of the International Committee on Taxonomy of 2020), which caused the SARS epidemic in 2002.

To combat COVID-19 one can use vaccines, antibodies and drugs. Currently, Pfizer, Moderna, AstraZeneca and other vaccines are widely used, but their side effects have not been fully studied and understood. Antibodies extracted from the plasma of recovered SARS-CoV-2 patients have valuable therapeutic effect (Jiang et al., 2020), but their quantity is small and quite expensive. Of the drugs available on the market, Remdesivir (Wang et al., 2020) and Dexamethasone (Group et al., 2021) have been found to be effective for critically ill patients, but their immune systems may get weaken (Khamisi, 2021). Molnupiravir (EIDD-2801/MK-4482), developed by Merck, is not FDA-approved, but it can reduce the risk of hospitalization or death in unvaccinated adults with COVID-19 (Jayk Bernal et al., 2022). Pfizer's

Paxlovid is the first drug approved by FDA for oral treatment for COVID-19 (Drożdżal et al., 2021), but like Molnupiravir, its ability to cope with emerging variants of concern such as Omicron (WHO, 2021) is under investigation. Thus, due to the limited number of drugs and drug candidates and an increasing number of variants of concern, the development of new drugs remains a challenge.

The human coronavirus genome encodes multiple structured proteins including spike (S), envelope (E), membrane (M), and nucleocapsid (N) proteins. It also contains non-structural proteins (NSPs) called NSP1 to NSP16 (Kim et al., 2020) (Figure 1). These proteins play a vital role in SARS-CoV-2 viral life cycle and emerge as promising targets for drug design studies (Arya et al., 2021; Huang et al., 2020; Nallagatla et al., 2008). Among them, the papain-like protease (PL^{PRO}) (NSP3) and the main protease (M^{PRO}) (NSP5), which play a crucial role in the regulation of various viral replication functions, have been intensively studied as drug targets (Jimenez-Alberto et al., 2020; Ma et al., 2021; Owen et al., 2021; Tripathi et al., 2020). Other studied targets are NSP12 (Elfiky 2021; Ruan et al., 2021), NSP13 (Perez-Lemus et al., 2022; White et al., 2020), NSP14 (Selvaraj et al., 2021), NSP15 (Sharma et al., 2022), NSP16 (El Hassab, Ibrahim, Al-Rashood, et al., 2021; El Hassab, Ibrahim; Shoun, et al., 2021; Jiang et al., 2022; Liang et al., 2021), spike (Kadioglu et al., 2021), nucleocapsid (Hu et al., 2021; Yadav et al., 2021), and

CONTACT Mai Suan  Limasli@ifpan.edu.pl  Institute of Physics, Polish Academy of Sciences, al. Lotnikow 32/46, Warsaw 02-668, Poland.

*These authors contributed equally.

 Supplemental data for this article can be accessed online at <https://doi.org/10.1080/07391102.2022.2114941>

© 2022 Informa UK Limited, trading as Taylor & Francis Group

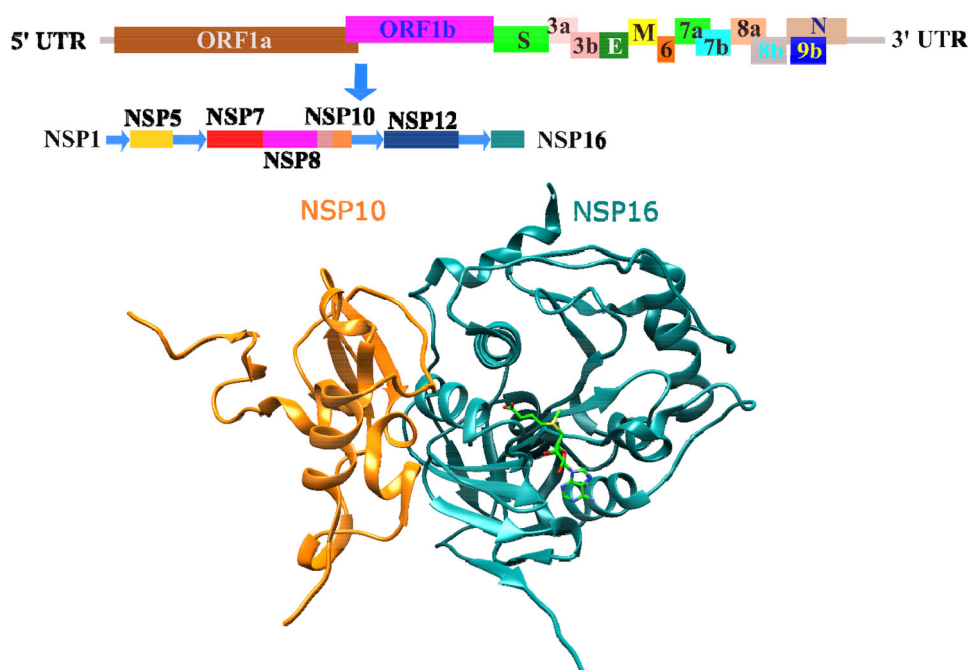


Figure 1. (Upper) Schematic description of SARS-CoV-2 RNA. (Lower) Structure of NSP16-NSP10 in complex with SAM molecule (PDB ID 6W4H).

envelope (Bhowmik et al., 2020; Orfali et al., 2021) proteins of SARS-CoV-2.

Coronavirus methyltransferases (MTases), nsp10/16 and nsp14, are SARS-CoV-2 enzymes that are crucial for RNA cap formation, an important process for viral RNA stability (Nencka et al., 2022). This function of MTase is tied to NSP16, which requires NSP10 as a cofactor to work properly (Bouvet et al., 2010; Kozielski et al., 2022; Krafcikova et al., 2020). Thus, the NSP16-NSP10 heterodimer becomes a potential target for antiviral therapy.

Through *in silico* screening Malik et al. (2021) found several potential inhibitors for NSP16-NSP10 5' methyl transferase activity from 128 phytocompounds and 11 FDA-approved HIV drugs. Maurya et al. (2020) performed a virtual screening of anti-viral, anti-infectious, and anti-protease compounds and found that telbivudine, oxytetracycline dihydrate, methylgalate, 2-deoxyglucose and daphnetin are the compounds that best bind to NSP10/NSP16 methyltransferase. Several inhibitors including those derived from SAH (S-adenosyl-L-homocysteine) were reported for this target (Bobijeva et al., 2021; Nencka, et al. 2022). Applying a pharmacophore modelling-based drug repurposing approach to the DrugBank database, several compounds (framycetin, kanamycin, tegobuvir, sonidegib, siramesine, antrafenine, and tobramycin) have been found as promising candidates for COVID-19 therapeutics (Encinar & Menendez, 2020; Rampogu & Lee, 2021). However, drug candidates inhibiting SARS-CoV-2 NSP16-N10 activity have not been identified from large databases. Therefore, here we attempted to search for potential inhibitors of this target from two large databases PubChem and anti-HIV using a multi-stage virtual screening (Figure 2).

NSP16-NSP10 structure deposited in the Protein Data Bank (PDB) was used as a drug target. A further reduction in the number of compounds was achieved by Lipinski's rule, molecular docking followed by steered molecular dynamics

(SMD) simulation (Thai et al., 2017). Finally, we performed umbrella sampling to estimate the binding free energy for the top two SMD-derived compounds from the two databases. This analysis indicated that PubChem's compound CID 135566620 is a good candidate for the treatment of COVID-19 as it has an inhibition constant IC₅₀ in the sub- μ M range.

2. Materials and methods

2.1. Target and ligands

The target is a complex of NSP16 and NSP10 and its structure was retrieved from PDB with the code 6W4H (Rosas-Lemus et al., 2020) (Figure 1). The binding site of this structure is known and coincides with the location of SAM (S-adenosyl methionine). Residues of NSP16 and NSP10 were renumbered, residue 1 of NSP16 in this work is 6799 from 6W4H, and residue 1 of NSP10 is 4271 from 6W4H.

The ligand structures were downloaded from two databases: PubChem database (Bolton et al., 2008) which comprises about 103 million compounds (Figure 2) and anti-HIV database of National Cancer Institute (NIAID Division of AIDS Anti-HIV/OI/TB Therapeutics Database, 2022) with 42,390 compounds collected in the 'AIDO99SD.BIN' file (Gasteiger, 2004).

2.2. Lipinski's rule

The first step in virtual screening is to apply Lipinski's rule of five (Lipinski et al., 1997) to obtain ligands with drug-like properties (Lipinski et al., 1997, 2012). According to this rule, a drug candidate should have a molecular weight from 0 to 500 Da, xlogP from 0 to 5, the number of donor hydrogen bonds from 0 to 5, and the number of acceptor hydrogen bonds from 0 to 10.

2.3. Docking simulation

Autodock Tool 1.5.4 (Morris et al., 2009; Sanner, 1999) in the package of MGL Tools-1.5.4 was used to convert the input PDB file to the PDBQT file format for docking a ligand to the target. The initial structures and parameters of the ligand and target for docking simulations were prepared using python scripts 'prepare_receptor4.py' and 'prepare_ligand4.py' plugged in Autodock Tool 1.5.4. Docking simulations were performed using Autodock Vina version 1.1.2 (Trott & Olson, 2010). For global search, the exhaustiveness parameter was set to 400, which is sufficient to obtain reliable results. The binding site of NSP16-NSP10 was known from experiment with the SAM (S-adenosyl methionine) ligand (Rosas-Lemus, et al. 2020) (Figure 1). To envelop just the binding site, a box with grid dimensions $20 \times 22 \times 22 \text{ \AA}$ was chosen. In docking simulations, the receptor dynamics was neglected, and the best docking mode with the lowest docking energy was selected.

To show that skipping receptor dynamics is acceptable, we ran docking simulations for 3 compounds from PubChem and 2 compounds from the HIV database where binding site residues are flexible and compare with the case of a rigid receptor. The binding energies in both cases are almost equal, but taking into account the receptor dynamics increases the simulation time by about 12–19 times (supplementary material Table S1). This result supports our choice to forego the flexibility of the receptor.

2.4. Molecular dynamics simulation

Molecular dynamics simulation was performed using the GROMACS 2020.2 package (Abraham et al., 2015) with an AMBER-f99SB-ILDN (Lindorff-Larsen et al., 2010) force field and TIP3P water model (Jorgensen et al., 1983). Note that the TIP3P water model is compatible with this force field (Lindorff-Larsen et al., 2010; Jorgensen et al., 1983) and has been successfully used in many previous works on protein-ligand association (Huy et al., 2014; Viet et al., 2015; Vuong et al., 2015; Zhang et al., 2021).

Force field parameters for ligands were calculated using Antechamber (Wang et al., 2001) and Acypype (Sousa da Silva & Vranken, 2012) derived from the General Amber Force Field (GAFF) (Wang et al., 2004). To obtain the point charge of atoms, a simple harmonic function form for bonds, angles and the AM1-BCC (Jakalian et al., 2000) charge model were used.

Complex systems were solvated in boxes filled with water molecules. Na^+ and Cl^- ions were added to neutralize the system and achieve a salt concentration of 0.15 M (Ali & Vijayan, 2020). Solvated systems contain about 130,000 atoms, of which about 41,600 are water molecules. The Van der Waals (vdW) force was calculated with a cut-off of 1.2 nm, while the particle-mesh Ewald summation method (Darden et al., 1993) was employed for calculating the electrostatic energy with the same cut-off as vdW. To solve the motion equation, a leapfrog algorithm (Hockney et al., 1974) with a time step of 0.2 fs was used.

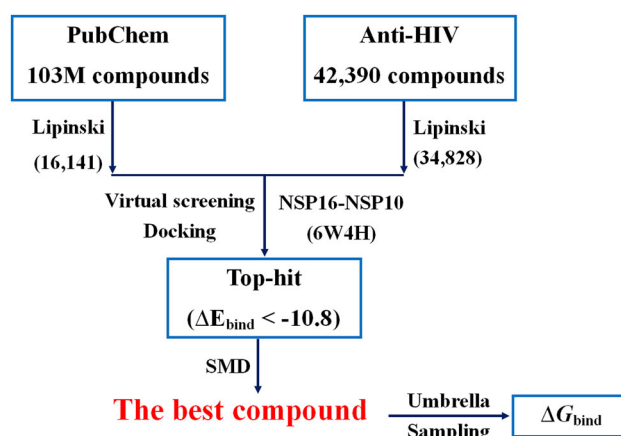


Figure 2. Multi-step screening procedure. Out of approximately 103 million (103 M) compounds of PubChem and 42,390 compounds of anti-HIV, we obtained 16,141 and 34,828 drug-like compounds after application of Lipinski's rule. Molecular docking, SMD and umbrella sampling were then used to identify the top compounds.

After energy minimization by the steepest descent method (Bartholomew-Biggs, 2005) and water molecules have entered the binding site, the system was equilibrated with position restraints on heavy atoms using a harmonic potential with a spring stiffness of $1000 \text{ kJ}/(\text{mol}\cdot\text{nm}^2)$ in NVT and NPT ensembles for MD simulations of 500 ps and 5 ns, respectively. Then, 50 ns conventional MD simulation was carried out for each system in NPT ensemble without restraints. The last snapshot obtained in this run will be used as the initial configuration for the SMD simulation. The v-rescale (Bussi et al., 2007) and Parrinello and Rahman (1981) algorithms were used to maintain temperature and pressure at 300 K and 1 atm during simulation, respectively.

2.5. SMD simulation

SMD can be employed to probe binding affinity by pulling a ligand out of a receptor binding site (Grubmuller et al., 1996). It has been recognized that SMD method is as accurate as the MM-PBSA method but computationally much faster due to fast pulling (Mai & Li, 2011; Suan Li & Khanh Mai, 2012; Vuong et al., 2015). Because the predictive power of the docking method is limited, the SMD is used to refine docking results in virtual screening as the next step in the multi-step screening procedure (Thai et al., 2017) (Figure 2).

In SMD, an external force is applied to a dummy atom that is linked to the ligand atom closest to the center of mass (COM) of the ligand by a spring with a stiffness k . Then the force experienced by the ligand is $F = k(\Delta x - vt)$, where v is the pulling speed and Δx is the pulled atom displacement from the initial position. As in AFM experiment (Gibson et al., 2007), we chose $k = 600 \text{ kJ}/(\text{mol}\cdot\text{nm}^2)$ and $v = 3 \text{ nm}/\text{ns}$ which was used previously (Mai & Li, 2011; Suan Li & Khanh Mai, 2012; Vuong et al., 2015). This value of v is about ten orders of magnitude larger than in the experiment, but as shown in previous works, this choice does not influence relative binding affinities, i.e., it can be used to discern strong binders from weak ones.

To prevent the receptor from drifting during pulling, we fixed the receptor C α -atoms located at a distance greater than the cut-off distance (1.2 nm) from the nearest ligand atom by applying a harmonic potential with a spring constant of 1000 kJ/(mol.nm²). This criterion was chosen because the interaction between pairs of atoms located farther than this distance is small.

The minimal steric hindrance (MSH) method (Vuong et al., 2015) was used to find the pulling direction that is the easiest path with the lowest rupture force F_{\max} (Mai et al., 2010). This path depends not only on the ligand but also on the SMD trajectory.

For each complex, five independent SMD runs of 1 ns were performed in the NPT ensemble. These runs are long enough to completely remove the ligand from the active site. In SMD either rupture force F_{\max} or the non-equilibrium work W_{pull} can be selected as a scoring function for ranking binding affinities. However, we will use the latter as it is more reliable (Vuong et al., 2015). W_{pull} is calculated as follows

$$W_{\text{pull}} = \int_0^{x_{\max}} \vec{F} \cdot d\vec{x} = \int_0^{T_{\max}} \vec{F} \frac{d\vec{x}}{dt} dt$$

$$\approx \sum_{i=1}^{N_{\text{step}}} \frac{(F_{i+1} + F_i)}{2} (x_{i+1} - x_i)$$

where F_i and x_i are the force and ligand displacement at SMD step i , respectively.

2.6. Umbrella sampling

Since the pulling work obtained with SMD at fast pulling can only be used to characterize the relative binding affinity, the absolute binding free energy ΔG should be estimated by other methods. In principle, ΔG can be calculated by combining SMD and the Jarzynski's equality (Hummer & Szabo, 2001; Jarzynski 1997) but this approach is impractical since a huge number of SMD runs are required (Park & Schulten, 2004). Therefore, umbrella sampling (US) (Torrie & Valleau, 1977) was used as it is one of the best MD-based methods for evaluating ΔG . Another reason for using US is that this method was successful in predicting the binding affinity of Remdesivir for SARS-CoV-2, as shown in our previous work (Nguyen et al., 2020).

One of the central issues of US is the suitable choice of the reaction coordinate for calculating the potential of mean force (PMF). Since the pulling was along the z-direction, the z coordinate of the ligand COM was chosen as the reaction coordinate for US (Figure 3). Because in the MSH scheme (Vuong et al., 2015) the pulling direction depends on the SMD trajectory, the pulling path of the trajectory is that it has a rupture force closest to the mean value of F_{\max} . $Z=0$ corresponds to the initial position of the ligand in the SMD simulation, while the maximum distance $z=2.8$ nm corresponds to the end of the simulation. To perform US simulations, this distance was divided into windows. For $0 \leq z \leq 0.8$ nm (blue part in Figure 3), where the receptor-ligand interaction is strong the width of the windows was set at 0.05 nm, and for $0.8 \text{ nm} < z \leq 2.8$ nm (red part in Figure 4)

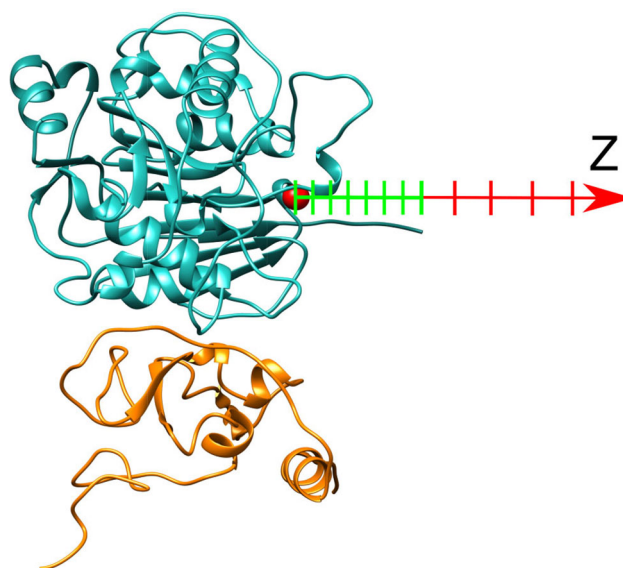


Figure 3. Setup for umbrella sampling with the reaction coordinate z . The red ball refers to the ligand in the binding site that correspond to $z=0$. Windows in the blue part of 0.8 nm have a width of 0.05 nm, while for the red part of 2 nm, a width of 0.1 nm was chosen.

the width of the windows was 0.1 nm. Thus, in total there are $0.8/0.05 + 2/0.1 = 36$ windows.

To not allow the ligand go far away from the window, we applied the harmonic potential

$$V_i = \frac{1}{2}k(z - z_i)^2$$

where $k = k_s = 600$ kJ/mol/nm², z_i is the center of window i . For each window, a 100 ns conventional MD simulation was carried out at 300 K and 1 bar.

Gmx WHAM (weight histogram analysis method) tool from GROMACS package was used for data analysis, and the error was calculated using the bootstrap method (Hub et al., 2010; Kumar et al., 1992).

2.7. Measures used in data analysis

The backbone root mean square deviation (RMSD) was used to measure the deviation of structure of the receptor from its initial configuration. A hydrogen bond (HB) was formed provided the distance between donor D and acceptor A is less than 3.5 Å, the H-A distance is less than 2.7 Å and the D-H-A angle is greater than 135 degrees. A non-bonded contact between the ligand and the receptor residue is formed if the distance between the ligand COM and COM of the side chain is less than 0.65 nm.

3. Results and discussions

3.1. Screening of drug-like compounds using Lipinski's rule

For the PubChem database applying Lipinski's rule (Lipinski, et al. 1997) reduced the number of ligands from 103 million to 16,140 (Figure 2). In the case of anti-HIV database, out of 42,390 compounds, 34,828 compounds are obtained. The

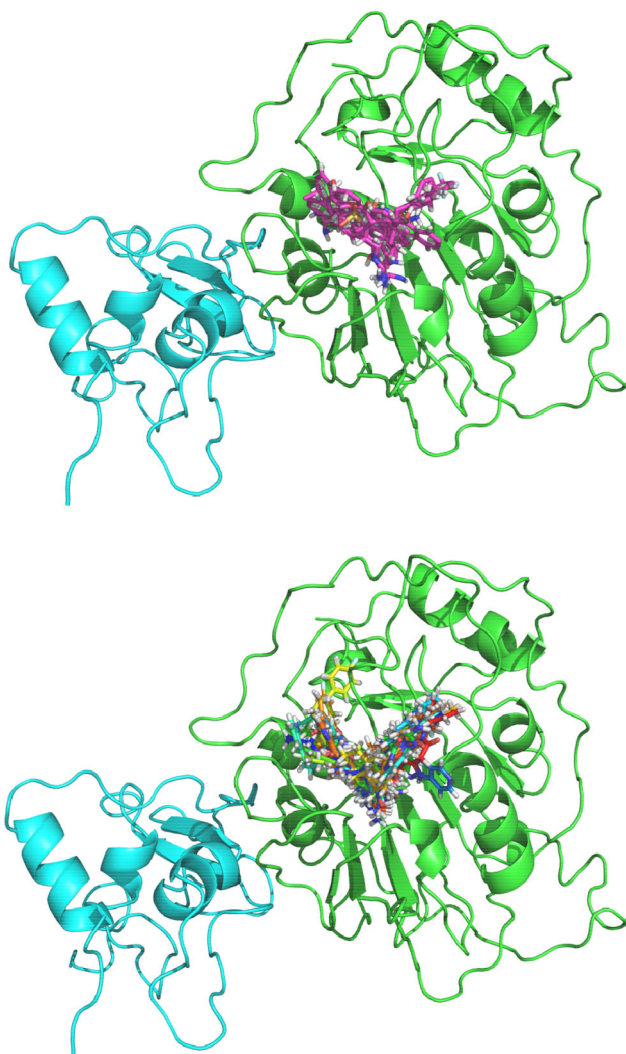


Figure 4. Binding positions of 6 compounds from the anti-HIV database (upper) and 19 compounds from the PubChem database (lower) with the binding energy below -10.8 kcal/mol. Results were obtained by docking simulation.

binding affinity of these drug-like compounds will be studied using the docking method in the next step.

3.2. Docking results

The Autodock Vina package was utilized to dock all compounds to the NSP16-NSP10 binding site. Binding energy distributions of compounds from anti-HIV and PubChem database are shown in Figure S1 in supplementary material. For the anti-HIV database, binding energies vary from -1.2 to -11.7 kcal/mol, while for the PubChem database, this range is shifted to $[-1.25, -12.0]$ kcal/mol. For both databases, the most populated energy is from -8.5 to -6.5 kcal/mol.

Restricting to compounds that have the docking energy less or equal -10.8 kcal/mol, 6 and 19 compounds are obtained from the anti-HIV and PubChem databases, respectively. We choose the cutoff of -10.8 kcal/mol because it guarantees an IC_{50} in the nM range (from the equation $\Delta G = R7\ln(IC_{50})$, it follows that $\Delta G = -10.8$ kcal/mol corresponds an IC_{50} of about 10 nM).

Three-dimensional structures and docking energies of the selected compounds are presented in supplementary material Table S2. The difference in their docking energies in both databases is insignificant. The top 6 and 19 compounds are located at the experimental binding site (Figure 4), indicating that they are promising candidates in terms of biological activity.

As shown below by SMD simulation, which is more reliable than the docking method, CID 135566620 ($E_{\text{dock}} = -10.9$ kcal/mol) and CID 20636 ($E_{\text{dock}} = -11.5$ kcal/mol) are the best of PubChem and anti-HIV databases, respectively. Therefore, these two compounds are considered in more detail as top leads for NSP16-NSP10. CID 135566620 forms only 1 hydrogen bond with 6W4H (supplementary material Figure S2), while CID 20636 forms 10 hydrogen bonds (supplementary material Figure S3).

CID 135566620 forms 12 non-bonded contacts with residues Gly71, Gly73, Ser74, Leu100, Asp114, Asp130, Met131, Tyr132, Thr136, Lys146, Gly148, and Phe149 of NSP16 (supplementary material Figure S2). CID 20636 has 8 non-bonded contacts with residues Ser98, Leu100, Asp99, Met131, Phe149, Pro134, Cys115, and Asp114 of NSP16 (supplementary material Figure S3). Thus, residues Leu100, Asp114, Met131, and Phe149 of NSP16 form non-bonded contact with both leads. These results also show that they have different interaction modes with NSP16-NSP10, because CID 20636 favours hydrogen bonding while CID 135566620 prefers non-bonded contacts. The experiment (Rosas-Lemus et al., 2020) showed that SAM binds to NSP16 at residues Asn43, Tyr47, Gly73, Gly81, Asp99, Leu100, Asn101, Asp114, Cys115, Asp130, Phe149 (Rosas-Lemus et al., 2020), indicating that, as mentioned above, these two compounds have the same binding site as SAM.

3.3. SMD results

We conducted SMD simulations for the top 6 and 19 compounds from anti-HIV and PubChem databases. Force and works profiles obtained for ID 135566620 (PubChem) and ID 20636 (anti-HIV) are shown in supplementary material Figure S4. Above the displacement of 2.5 nm the pulling work becomes saturated. Therefore, we defined W_{pull} as work at the end of a simulation.

The results obtained for F_{max} and W_{pull} averaged over five independent runs are presented in Table 1. The best ligands CID 135566620 and CID 20636 have similar pulling work of 87.0 ± 2.2 and 83.8 ± 2.5 kcal/mol. This is also true for the rupture force F_{max} . Note that in terms of docking energy, CID 20636 is second in the anti-HIV database (Table 1), while CID 135566620 is 11th in the PubChem database, which may be due to the fact that the top 19 compounds in this database have approximately the same docking energy.

W_{pull} of the weakest ligands of the two databases is 29.9 ± 2.3 (CID 361242) and 27.2 ± 1.3 kcal/mol (CID 134812662) (Table 1). Although the difference between the docking energies of the best and worst ligands in these databases is negligible, the difference in pulling works is notable, suggesting that the docking method is less sensitive than SMD.

The pulling work of the second-ranked compound in the anti-HIV database (59.7 ± 3.8 kcal/mol) is equivalent only to

Table 1. SMD results for the top compounds identified by docking simulation.

Database	rank	ID	Work (kcal/mol)	F_{max} (pN)
Anti-HIV activity	1	20636	83.8 ± 2.5	867.2 ± 22.1
	2	632036	59.7 ± 3.8	599.0 ± 31.7
	3	5268	40.6 ± 2.5	398.9 ± 28.0
	4	633240	39.1 ± 3.7	408.1 ± 23.9
	5	682768	34.0 ± 2.1	388.1 ± 31.1
	6	361242	29.9 ± 2.3	324.8 ± 20.6
PubChem	1	135566620	87.0 ± 2.2	844.7 ± 55.1
	2	58540191	71.6 ± 1.8	691.4 ± 53.7
	3	57842673	69.2 ± 4.4	719.9 ± 55.4
	4	135566329	64.1 ± 4.9	612.9 ± 49.2
	5	6539952	60.7 ± 4.3	598.8 ± 25.5
	6	71009649	55.9 ± 3.0	555.3 ± 55.2
	7	58829329	54.4 ± 2.9	581.4 ± 74.3
	8	131801415	52.3 ± 2.7	481.8 ± 22.5
	9	66604359	49.7 ± 2.5	544.8 ± 33.2
	10	71296047	47.7 ± 2.8	485.4 ± 49.3
	11	71296046	47.3 ± 1.9	488.8 ± 67.9
	12	134812663	45.1 ± 2.4	473.6 ± 35.3
	13	23646856	44.5 ± 5.6	437.9 ± 66.7
14	117996541	44.2 ± 2.7	453.9 ± 16.5	
15	134812664	36.3 ± 2.7	97.6 ± 46.6	
16	15991573	35.7 ± 1.7	511.5 ± 34.6	
17	24916755	33.8 ± 1.7	401.7 ± 52.0	
18	44593854	33.6 ± 3.6	365.8 ± 60.6	
19	134812662	27.2 ± 1.3	332.9 ± 25.1	

The best compounds of two databases are in bold. Results were averaged over five trajectories.

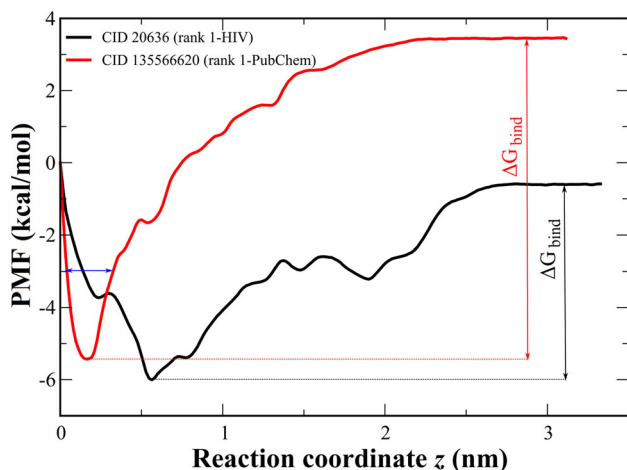


Figure 5. Dependence of potential of mean force (PMF) on reaction coordinate z of two best compounds from the anti-HIV and PubChem databases. Black and red arrows represent binding free energies. Snapshots collected in the state with PMF under the blue arrow were used to analyze the binding mechanism of CID 135566620.

the top 4 (64.1 ± 4.9 kcal/mol) and top 5 (60.7 ± 4.3 kcal/mol) in the PubChem database (Table 1), showing that PubChem contains more compounds with strong binding affinity with NSP10-NSP16 than the anti-HIV database. However, this conclusion was drawn using the criteria we developed and may not be valid for other cases. We will calculate the absolute binding free energy of the best compounds CID 135566620 and CID 20636 using US.

3.4. Binding free energy from umbrella sampling: CID 135566620 is the top compound

Using US method, we obtained PMF for two best compounds chosen from SMD simulations (Figure 5). From the

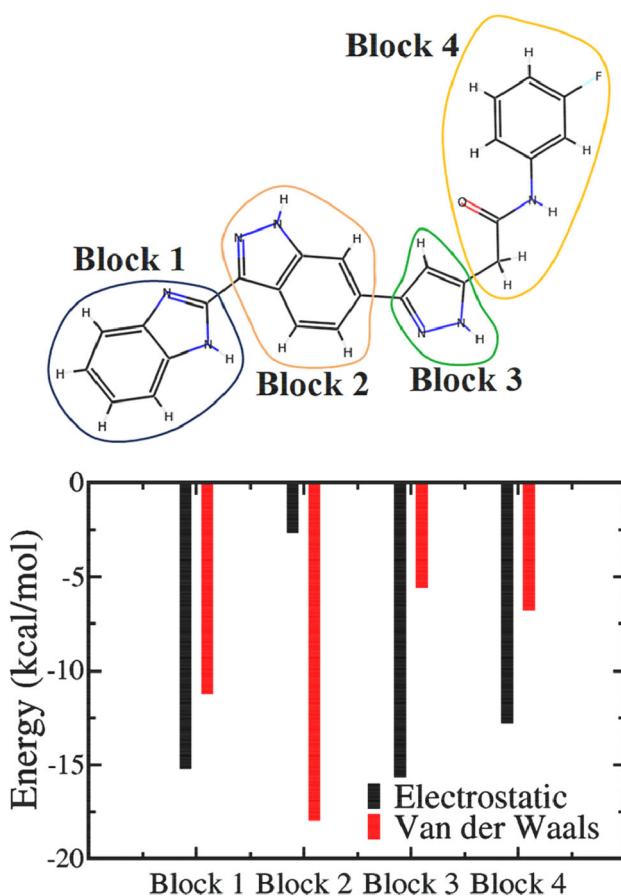


Figure 6. (Upper) CID 135566620 is divided into four blocks. (Below) Average interaction energy of 4 blocks with NSP16-NSP10 in the bound state. Results were obtained using US.

PMF profiles, we obtained the binding free energy $\Delta G = -8.89 \pm 0.81$ and -6.73 ± 0.42 kcal/mol for CID 135566620 and CID 20636, respectively. Using equation $IC_{50} = \exp(\Delta G/(RT))$ with $RT = 0.597$ kcal/mol at 300 K and IC_{50} measured in M, we obtained $IC_{50} \approx 0.34 \mu M$ and $12.7 \mu M$ for top leads from the PubChem and anti-HIV databases, respectively. We also performed US for the second best compound CID 58540191 from the PubChem database (Table 1) and obtained $\Delta G = -4.79 \pm 0.79$ kcal/mol, which is significantly higher than that of CID 135566620 and CID 20636. Therefore, US simulation was not carried out for other compounds in Table 1.

The experiment found that IC_{50} of inhibitors sinefungin, AdoHcy, and ATA for NSP16-NSP10 of the old SARS-CoV is 0.736 ± 0.71 , 12 ± 1.9 , and $2.1 \pm 0.2 \mu M$, respectively (Bouvet et al., 2010), which suggest that the binding affinity of these compounds to SARS-CoV is lower than that of the top lead from the PubChem database for SARS-CoV-2 NSP16. Since these compounds have been shown to be able to inhibit SARS-CoV replication (Bouvet et al., 2010; He et al., 2004), we expect that CID 135566620 can block the activity of SARS-CoV-2 through binding to NSP16-NSP10. Therefore, CID 135566620 found in this work is a promising inhibitor for SARS-CoV-2 NSP16-NSP10 as its IC_{50} is in the sub- μM range. Note that this compound binds to NSP16-NSP10 more strongly than SAM, which has the experimental value of the dissociation constant K_d of $37 \mu M$ (Viswanathan et al., 2020).

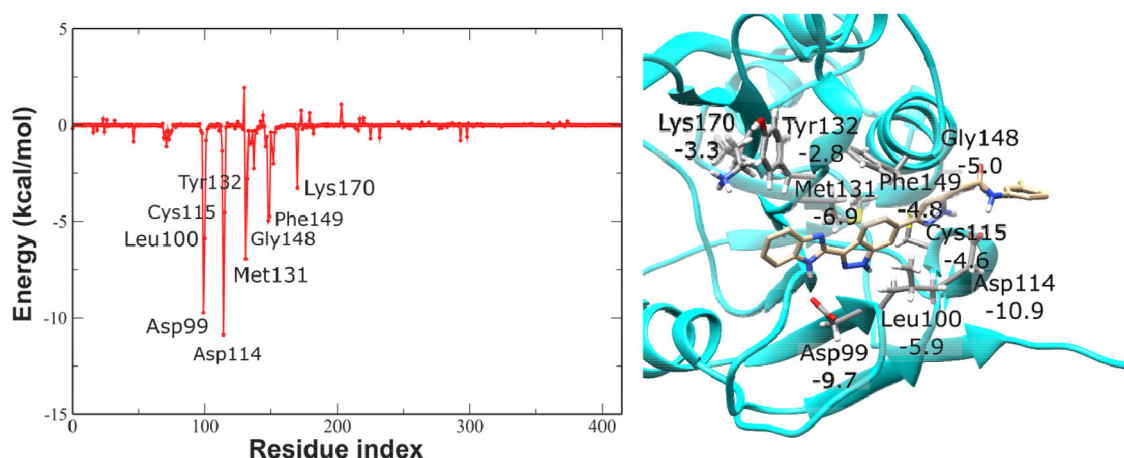


Figure 7. (Left) Non-bonded interaction energy of the residues of NSP10-NSP16 and CID 135566620. The NSP10 residue index is from 300 to 415, NSP16 is from 1 to 299. Shown are residues that have a non-bonded energy less than or equal to -2.5 kcal/mol. (Right) Schematic of residues presented in the left part with non-bonded energy shown below the label. Results were obtained by using US.

3.5. Binding mechanism of CID 135566620: vdW interaction is more important than the electrostatic interaction

Since CID 135566620 is the top lead, we examined its binding mechanism with NSP16-NSP10 in detail using data obtained from US (SMD data were not considered as they were obtained out of equilibrium). We adopted the same residue numbering as in Krafcikova et al. (2020). To study the receptor-ligand interaction in the bound state we used the configurations obtained in US trajectories in the region below the blue arrow in Figure 5. The electrostatic and vdW interaction energies between NSP16-NSP10 and CID 135566620 are -33.39 ± 0.19 and -40.59 ± 0.90 kcal/mol, respectively, indicating that the vdW interaction is more important than the electrostatic interaction.

To understand the role of different groups of atoms, we divided the ligand into 4 blocks: block 1-1H-benzo[d]imidazole, block 2-1H-indazole, block 3-1H-pyrazole and block 4-N-(3-fluorophenyl) acetamide (Figure 6). The total interaction energy (vdW plus electrostatic) of the blocks is -24.15 , -17.48 , -13.26 , and -19.07 kcal/mol, respectively (Figure 6), which means that block 1 makes the greatest contribution to the stability of the complex. For block 2, the vdW interaction prevails, while for blocks 1 and 3 the opposite takes place. For block 4 two types of interaction are compatible.

Residues Asp99, Leu100, Asp114, Cys115, Met131, Tyr132, Gly148, Phe149, Lys170 of NSP16 have the strong non-bonded interaction with the ligand (Figure 7). Among them, Asp114 and Asp99 of NSP16 are the most important as they have the interaction energy of -10.9 and -9.7 kcal/mol.

Met131 and Lys170 do not form a hydrogen bond with CID 135566620, unlike other residues (supporting material Figure S5). Asp99, Asp114, Cys115, and Tyr132 have significant population of HBs in excess of 10%, suggesting that CID135566620 interacts with NSP16-NSP10 primarily through non-bonded interaction and hydrogen bonding.

4. Conclusions

Using the multi-step screening procedure including Lipinski's rule, docking, SMD and umbrella sampling, we identified CID

135566620 from the PubChem database as the most promising compound to inhibit NSP16-NSP10 activity. Its binding free energy is -8.89 kcal/mol, which corresponds to $IC_{50} \approx 0.34$ μ M. We have provided mechanistic insights into the binding mechanism of the top lead, showing that both electrostatic and vdW interactions contribute, but the role of the vdW interaction is more significant. In addition, 1H-benzo[d]imidazole group (block 1) of CID 135566620, which has the lowest interaction energy with NSP16-NSP10, plays a crucial role in the stability of the complex.

It can be expected that in the presence of CID 135566620, SARS-COV-2 replication slows down. Therefore, CID 13556 is recommended for further *in vitro* and *in vivo* studies.

Disclosure statement

The authors declare no competing financial interest.

Funding

This work was supported by Narodowe Centrum Nauki in Poland (Grant 2019/35/B/ST4/02086), the Department of Science and Technology at Ho Chi Minh city (Grant 45/2020/HD-QPTKHCN), the TASK Supercomputer Center in Gdansk, PLGrid Infrastructure, Poland and the HPCC at the Institute for Computational Science and Technology, Ho Chi Minh City, Vietnam. Hoang Linh Nguyen was funded by Vingroup JSC and supported by the Master, PhD Scholarship Programme of Vingroup Innovation Foundation (VINIF), Institute of Big Data, code VINIF.2021.TS.029.

ORCID

Mai Suan Li  <http://orcid.org/0000-0001-7021-7916>

References

Abraham, M. J., Murtola, T., Schulz, R., Páll, S., Smith, J. C., Hess, B., & Lindahl, E. (2015). GROMACS: High performance molecular simulations through multi-level parallelism from laptops to supercomputers. *SoftwareX*, 1–2, 19–25. <https://doi.org/10.1016/j.softx.2015.06.001>

- Ali, A., & Vijayan, R. (2020). Dynamics of the ACE2–SARS-CoV-2/SARS-CoV spike protein interface reveal unique mechanisms. *Scientific Reports*, 10(1), 14214. <https://doi.org/10.1038/s41598-020-71188-3>
- Arya, R., Kumari, S., Pandey, B., Mistry, H., Bihani, S. C., Das, A., Prashar, V., Gupta, G. D., Panicker, L., & Kumar, M. (2021). Structural insights into SARS-CoV-2 proteins. *Journal of Molecular Biology*, 433(2), 166725. <https://doi.org/10.1016/j.jmb.2020.11.024>
- Bartholomew-Biggs, M. (2005). The steepest descent method. In: *Nonlinear optimization with financial applications* (pp. 51–64). Springer. https://doi.org/10.1007/0-387-24149-3_5
- Bhowmik, D., Nandi, R., Jagadeesan, R., Kumar, N., Prakash, A., & Kumar, D. (2020). Identification of potential inhibitors against SARS-CoV-2 by targeting proteins responsible for envelope formation and virion assembly using docking based virtual screening, and pharmacokinetics approaches. *Infection, Genetics and Evolution*, 84, 104451. <https://doi.org/10.1016/j.meegid.2020.104451>
- Bobiljeva, O., Bobrovs, R., Kanēpe, I., Patetko, L., Kalniņš, G., Šišovs, M., Bula, A. L., Gri Nberga, S., Boroduškis, M. R., Ramata-Stunda, A., Rostoks, N., Jirgensons, A., Ta Rs, K., & Jaudzems, K. (2021). Potent SARS-CoV-2 mRNA cap methyltransferase inhibitors by bioisosteric replacement of methionine in SAM cosubstrate. *ACS Medicinal Chemistry Letters*, 12(7), 1102–1107. <https://doi.org/10.1021/acsmchemlett.1c00140>
- Bolton, E. E., Wang, Y., Thiessen, P. A., & Bryant, S. H. (2008). Chapter 12 - PubChem: Integrated platform of small molecules and biological activities. *Annual Reports in Computational Chemistry*, 4, 217–241. [https://doi.org/10.1016/S1574-1400\(08\)00012-1](https://doi.org/10.1016/S1574-1400(08)00012-1)
- Bouvet, M., Debarnot, C., Imbert, I., Selisko, B., Snijder, E. J., Canard, B., & Decroly, E. (2010). In vitro reconstitution of SARS-coronavirus mRNA cap methylation. *PLoS Pathogens*, 6(4), e1000863. <https://doi.org/10.1371/journal.ppat.1000863>
- Bussi, G., Donadio, D., & Parrinello, M. (2007). Canonical sampling through velocity rescaling. *The Journal of Chemical Physics*, 126(1), 014101. <https://doi.org/10.1063/1.2408420>
- Coronaviridae Study Group of the International Committee on Taxonomy of Viruses. (2020). The species severe acute respiratory syndrome-related coronavirus: classifying 2019-nCoV and naming it SARS-CoV-2. *Nature Microbiology*, 5(4), 536–544. <https://doi.org/10.1038/s41564-020-0695-z>
- Darden, T., York, D., & Pedersen, L. (1993). Particle mesh Ewald: An N-log(N) method for Ewald sums in large systems. *The Journal of Chemical Physics*, 98(12), 10089–10092. <https://doi.org/10.1063/1.464397>
- El Hassab, M. A., Ibrahim, T. M., Al-Rashood, S. T., Alharbi, A., Eskandrani, R. O., & Eldehna, W. M. (2021). In silico identification of novel SARS-CoV-2 2'-O-methyltransferase (nsp16) inhibitors: structure-based virtual screening, molecular dynamics simulation and MM-PBSA approaches. *Journal of Enzyme Inhibition and Medicinal Chemistry*, 36(1), 727–736. <https://doi.org/10.1080/14756366.2021.1885396>
- El Hassab, M. A., Ibrahim, T. M., Shoun, A. A., Al-Rashood, S. T., Alkahtani, H. M., Alharbi, A., Eskandrani, R. O., & Eldehna, W. M. (2021). In silico identification of potential SARS COV-2 2'-O-methyltransferase inhibitor: fragment-based screening approach and MM-PBSA calculations. *RSC Advances*, 11(26), 16026–16033. <https://doi.org/10.1039/d1ra01809d>
- Elfiky, A. A. (2021). SARS-CoV-2 RNA dependent RNA polymerase (RdRp) targeting: an in silico perspective. *Journal of Biomolecular Structure & Dynamics*, 39(9), 3204–3212. <https://doi.org/10.1080/07391102.2020.1761882>
- Encinar, J. A., & Menendez, J. A. (2020). Potential drugs targeting early innate immune evasion of SARS-coronavirus 2 via 2'-O-methylation of viral RNA. *Viruses*, 12(5), 525. <https://doi.org/10.3390/v12050525>
- AIDS Antiviral Screen Data. (Sep 08, 2021). <https://wiki.nci.nih.gov/display/NCIDTPdata/AIDS+Antiviral+Screen+Data>
- Gasteiger's group (2004). AIDS Antiviral Screen Data. Available from <https://wiki.nci.nih.gov/display/NCIDTPdata/AIDS+Antiviral+Screen+Data>
- Gibson, C. T., Carnally, S., & Roberts, C. J. (2007). Attachment of carbon nanotubes to atomic force microscope probes. *Ultramicroscopy*, 107(10–11), 1118–1122. <https://doi.org/10.1016/j.ultramic.2007.02.045>
- Group, R. C., Horby, P., Lim, W. S., Emberson, J. R., Mafham, M., Bell, J. L., Linsell, L., Staplin, N., Brightling, C., & Ustianowski, A. (2021). Dexamethasone in hospitalized patients with Covid-19. *The New England Journal of Medicine*, 384(8), 693–704. <https://doi.org/10.1056/NEJMoa2021436>
- Grubmuller, H., Heymann, B., & Tavan, P. (1996). Ligand binding: molecular mechanics calculation of the streptavidin-biotin rupture force. *Science (New York, NY)*, 271(5251), 997–999. <https://doi.org/10.1126/science.271.5251.997>
- He, R., Adonov, A., Traykova-Adonova, M., Cao, J., Cutts, T., Grudsky, E., Deschambaul, Y., Berry, J., Drobot, M., & Li, X. (2004). Potent and selective inhibition of SARS coronavirus replication by aurintricarboxylic acid. *Biochemical and Biophysical Research Communications*, 320(4), 1199–1203. <https://doi.org/10.1016/j.bbrc.2004.06.076>
- Hockney, R., Goel, S., & Eastwood, J. (1974). Quiet high-resolution computer models of a plasma. *Journal of Computational Physics*, 14(2), 148–158. [https://doi.org/10.1016/0021-9991\(74\)90010-2](https://doi.org/10.1016/0021-9991(74)90010-2)
- Hu, X., Zhou, Z., Li, F., Xiao, Y., Wang, Z., Xu, J., Dong, F., Zheng, H., & Yu, R. (2021). The study of antiviral drugs targeting SARS-CoV-2 nucleocapsid and spike proteins through large-scale compound repurposing. *Heliyon*, 7(3), e06387. <https://doi.org/10.1016/j.heliyon.2021.e06387>
- Huang, Y., Yang, C., Xu, X. F., Xu, W., & Liu, S. W. (2020). Structural and functional properties of SARS-CoV-2 spike protein: Potential antiviral drug development for COVID-19. *Acta Pharmacologica Sinica*, 41(9), 1141–1149. <https://doi.org/10.1038/s41401-020-0485-4>
- Hub, J. S., de Groot, B. L., & van der Spoel, D. (2010). g_wham—A free weighted histogram analysis implementation including robust error and autocorrelation estimates. *Journal of Chemical Theory and Computation*, 6(12), 3713–3720. <https://doi.org/10.1021/ct100494z>
- Hummer, G., & Szabo, A. (2001). Free energy reconstruction from nonequilibrium single-molecule pulling experiments. *Proceedings of the National Academy of Sciences of the United States of America*, 98(7), 3658–3661. <https://doi.org/10.1073/pnas.071034098>
- Huy, P. D. Q., & Li, M. S. (2014). Binding of fullerenes to amyloid beta fibrils: Size matters. *Physical Chemistry Chemical Physics*, 16(37), 20030–20040. <https://doi.org/10.1039/C4CP02348J>
- Jakalian, A., Bush, B. L., Jack, D. B., & Bayly, C. I. (2000). Fast, efficient generation of high-quality atomic charges. AM1-BCC model: I. Method. *Journal of Computational Chemistry*, 21(2), 132–146. <https://doi.org/10.1002/jcc.10128>
- Jarzynski, C. (1997). Nonequilibrium equality for free energy differences. *Physical Review Letters*, 78(14), 2690–2693. <https://doi.org/10.1103/PhysRevLett.78.2690>
- Jayk Bernal, A., Gomes da Silva, M. M., Musungaie, D. B., Kovalchuk, E., Gonzalez, A., Delos Reyes, V., Martín-Quirós, A., Caraco, Y., Williams-Diaz, A., Brown, M. L., Du, J., Pedley, A., Assaid, C., Strizki, J., Grobler, J. A., Shamsuddin, H. H., Tipping, R., Wan, H., Paschke, A., ... De Anda, C. (2022). Molnupiravir for oral treatment of covid-19 in nonhospitalized patients. *New England Journal of Medicine*, 386(6), 509–520. <https://doi.org/10.1056/NEJMoa2116044>
- Jiang, S., Hillyer, C., & Du, L. (2020). Neutralizing antibodies against SARS-CoV-2 and other human coronaviruses. *Trends in Immunology*, 41(5), 355–359. <https://doi.org/10.1016/j.it.2020.03.007>
- Jiang, Y., Liu, L., Manning, M., Bonahoom, M., Lotvola, A., Yang, Z., & Yang, Z. Q. (2022). Structural analysis, virtual screening and molecular simulation to identify potential inhibitors targeting 2'-O-ribose methyltransferase of SARS-CoV-2 coronavirus. *Journal of Biomolecular Structure & Dynamics*, 40(3), 1331–1346. <https://doi.org/10.1080/07391102.2020.1828172>
- Jimenez-Alberto, A., Ribas-Aparicio, R. M., Aparicio-Ozores, G., & Castelan-Vega, J. A. (2020). Virtual screening of approved drugs as potential SARS-CoV-2 main protease inhibitors. *Computational Biology and Chemistry*, 88, 107325. <https://doi.org/10.1016/j.compbiolchem.2020.107325>
- Jorgensen, W. L., Chandrasekhar, J., Madura, J. D., Impey, R. W., & Klein, M. L. (1983). Comparison of simple potential functions for simulating liquid water. *The Journal of Chemical Physics*, 79(2), 926–935. <https://doi.org/10.1063/1.445869>
- Kadioglu, O., Saeed, M., Greten, H. J., & Efferth, T. (2021). Identification of novel compounds against three targets of SARS CoV-2 coronavirus by

- combined virtual screening and supervised machine learning. *Computers in Biology and Medicine*, 133, 104359. <https://doi.org/10.1016/j.compbiomed.2021.104359>
- Khamsi, R. (2021). Rogue antibodies could be driving severe COVID-19. *Nature*, 590(7844), 29–31. <https://doi.org/10.1038/d41586-021-00149-1>
- Kim, D., Lee, J. Y., Yang, J. S., Kim, J. W., Kim, V. N., & Chang, H. (2020). The architecture of SARS-CoV-2 transcriptome. *Cell*, 181(4), 914–921. <https://doi.org/10.1016/j.cell.2020.04.011>
- Kozielski, F., Sele, C., Talibov, V. O., Lou, J., Dong, D., Wang, Q., Shi, X., Nyblom, M., Rogstam, A., Krojer, T., Fisher, Z., & Knecht, W. (2022). Identification of fragments binding to SARS-CoV-2 nsp10 reveals ligand-binding sites in conserved interfaces between nsp10 and nsp14/nsp16. *RSC Chemical Biology*, 3(1), 44–55. <https://doi.org/10.1039/D1CB00135C>
- Krafcikova, P., Silhan, J., Nencka, R., & Boura, E. (2020). Structural analysis of the SARS-CoV-2 methyltransferase complex involved in RNA cap creation bound to sinefungin. *Nature Communications*, 11(1), 3717. <https://doi.org/10.1038/s41467-020-17495-9>
- Kumar, S., Rosenberg, J. M., Bouzida, D., Swendsen, R. H., & Kollman, P. A. (1992). THE weighted histogram analysis method for free-energy calculations on biomolecules. I. The method. *Journal of Computational Chemistry*, 13(8), 1011–1021. <https://doi.org/10.1002/jcc.540130812>
- Liang, J., Pitsillou, E., Burbury, L., Hung, A., & Karagiannis, T. C. (2021). In silico investigation of potential small molecule inhibitors of the SARS-CoV-2 nsp10-nsp16 methyltransferase complex. *Chemical Physics Letters*, 774, 138618. <https://doi.org/10.1016/j.cplett.2021.138618>
- Lindorff-Larsen, K., Piana, S., Palmo, K., Maragakis, P., Klepeis, J. L., Dror, R. O., & Shaw, D. E. (2010). Improved side-chain torsion potentials for the Amber ff99SB protein force field. *Proteins*, 78(8), 1950–1958. <https://doi.org/10.1002/prot.22711>
- Lipinski, C. A., Lombardo, F., Dominy, B. W., & Feeney, P. J. (2012). Experimental and computational approaches to estimate solubility and permeability in drug discovery and development settings. *Advanced Drug Delivery Reviews*, 64, 4–17. <https://doi.org/10.1016/j.addr.2012.09.019>
- Lipinski, C. A., Lombardo, F., Dominy, B. W., & Feeney, P. J. (1997). Experimental and computational approaches to estimate solubility and permeability in drug discovery and development settings. *Advanced Drug Delivery Reviews*, 23(1–3), 3–25. [https://doi.org/10.1016/S0169-409X\(96\)00423-1](https://doi.org/10.1016/S0169-409X(96)00423-1)
- Ma, C., Sacco, M. D., Xia, Z., Lambrinidis, G., Townsend, J. A., Hu, Y., Meng, X., Szeto, T., Ba, M., Zhang, X., Gongora, M., Zhang, F., Marty, M. T., Xiang, Y., Kolocouris, A., Chen, Y., & Wang, J. (2021). Discovery of SARS-CoV-2 papain-like protease inhibitors through a combination of high-throughput screening and a FlipGFP-based reporter assay. *ACS Central Science*, 7(7), 1245–1260. <https://doi.org/10.1021/acscentsci.1c00519>
- Mai, B. K., & Li, M. S. (2011). Neuraminidase inhibitor R-125489–A promising drug for treating influenza virus: steered molecular dynamics approach. *Biochemical and Biophysical Research Communications*, 410(3), 688–691. <https://doi.org/10.1016/j.bbrc.2011.06.057>
- Mai, B. K., Viet, M. H., & Li, M. S. (2010). Top leads for swine influenza A/H1N1 virus revealed by steered molecular dynamics approach. *Journal of Chemical Information and Modeling*, 50(12), 2236–2247. <https://doi.org/10.1021/ci100346s>
- Malik, A., Kohli, M., Jacob, N. A., Kayal, A., Raj, T. K., Kulkarni, N., & Chandramohan, V. (2021). In silico screening of phytochemical compounds and FDA drugs as potential inhibitors for NSP16/10 5' methyltransferase activity. *Journal of Biomolecular Structure and Dynamics*, 1–13. <https://doi.org/10.1080/07391102.2021.2005680>
- Maurya, S. K., Maurya, A. K., Mishra, N., & Siddique, H. R. (2020). Virtual screening, ADME/T, and binding free energy analysis of anti-viral, anti-protease, and anti-infectious compounds against NSP10/NSP16 methyltransferase and main protease of SARS CoV-2. *Journal of Receptor and Signal Transduction Research*, 40(6), 605–612. <https://doi.org/10.1080/10799893.2020.1772298>
- Morris, G. M., Huey, R., Lindstrom, W., Sanner, M. F., Belew, R. K., Goodsell, D. S., & Olson, A. J. (2009). AutoDock4 and AutoDockTools4: Automated docking with selective receptor flexibility. *Journal of Computational Chemistry*, 30(16), 2785–2791. <https://doi.org/10.1002/jcc.21256>
- Nallagatla, S. R., Toroney, R., & Bevilacqua, P. C. (2008). A brilliant disguise for self RNA: 5'-end and internal modifications of primary transcripts suppress elements of innate immunity. *RNA Biology*, 5(3), 140–144. <https://doi.org/10.4161/rna.5.3.6839>
- Nencka, R., Silhan, J., Klima, M., Otava, T., Kocek, H., Krafcikova, P., & Boura, E. (2022). Coronaviral RNA-methyltransferases: function, structure and inhibition. *Nucleic Acids Research*, 50(2), 635–650. <https://doi.org/10.1093/nar/gkab1279>
- Nguyen, H. L., Thai, N. Q., Truong, D. T., & Li, M. S. (2020). Remdesivir strongly binds to both RNA-dependent RNA polymerase and main protease of SARS-CoV-2: Evidence from molecular simulations. *The Journal of Physical Chemistry B*, 124(50), 11337–11348. <https://doi.org/10.1021/acs.jpcc.0c07312>
- NIAID Division of AIDS Anti-HIV/OI/TB Therapeutics Database. <https://chemdb.niaid.nih.gov/>
- Orfali, R., Rateb, M. E., Hassan, H. M., Alonazi, M., Gomaa, M. R., Mahrous, N., GabAllah, M., Kandeil, A., Perveen, S., Abdelmohsen, U. R., & Sayed, A. M. (2021). Sinapic acid suppresses SARS CoV-2 replication by targeting its envelope protein. *Antibiotics (Basel)*, 10(4), 420. <https://doi.org/10.3390/antibiotics10040420>
- Owen, D. R., Allerton, C. M. N., Anderson, A. S., Aschenbrenner, L., Avery, M., Berritt, S., Boras, B., Cardin, R. D., Carlo, A., Coffman, K. J., Dantonio, A., Di, L., Eng, H., Ferre, R., Gajiwala, K. S., Gibson, S. A., Greasley, S. E., Hurst, B. L., Kadar, E. P., ... Zhu, Y. (2021). An oral SARS-CoV-2 M(pro) inhibitor clinical candidate for the treatment of COVID-19. *Science (New York, NY)*, 374(6575), 1586–1593. <https://doi.org/10.1126/science.abl4784>
- Park, S., & Schulten, K. (2004). Calculating potentials of mean force from steered molecular dynamics simulations. *The Journal of Chemical Physics*, 120(13), 5946–5961. <https://doi.org/10.1063/1.1651473>
- Parrinello, M., & Rahman, A. (1981). Polymorphic transitions in single crystals: A new molecular dynamics method. *Journal of Applied Physics*, 52(12), 7182–7190. <https://doi.org/10.1063/1.328693>
- Perez-Lemus, G. R., Menendez, C. A., Alvarado, W., Bylehn, F., & de Pablo, J. J. (2022). Toward wide-spectrum antivirals against coronaviruses: Molecular characterization of SARS-CoV-2 NSP13 helicase inhibitors. *Science Advances*, 8(1), eabj4526. <https://doi.org/10.1126/sciadv.abj4526>
- Rampogu, S., & Lee, K. W. (2021). Pharmacophore modelling-based drug repurposing approaches for SARS-CoV-2 therapeutics. *Frontiers in Chemistry*, 9, 636362. <https://doi.org/10.3389/fchem.2021.636362>
- Rosas-Lemus, M., Minasov, G., Shuvalova, L., Inniss, N. L., Kiryukhina, O., Brunzelle, J., & Satchell, K. J. F. (2020). High-resolution structures of the SARS-CoV-2 2'-O-methyltransferase reveal strategies for structure-based inhibitor design. *Science Signaling*, 13(651), eabe1202. <https://doi.org/10.1126/scisignal.abe1202>
- Ruan, Z., Liu, C., Guo, Y., He, Z., Huang, X., Jia, X., & Yang, T. (2021). SARS-CoV-2 and SARS-CoV: Virtual screening of potential inhibitors targeting RNA-dependent RNA polymerase activity (NSP12). *Journal of Medical Virology*, 93(1), 389–400. <https://doi.org/10.1002/jmv.26222>
- Sanner, M. F. (1999). Python: a programming language for software integration and development. *Journal of Molecular Graphics & Modelling*, 17(1), 57–61.
- Selvaraj, C., Dinesh, D. C., Panwar, U., Abhirami, R., Boura, E., & Singh, S. K. (2021). Structure-based virtual screening and molecular dynamics simulation of SARS-CoV-2 Guanine-N7 methyltransferase (nsp14) for identifying antiviral inhibitors against COVID-19. *Journal of Biomolecular Structure & Dynamics*, 39(13), 4582–4593. <https://doi.org/10.1080/07391102.2020.1778535>
- Sharma, A., Goyal, S., Yadav, A. K., Kumar, P., & Gupta, L. (2022). In-silico screening of plant-derived antivirals against main protease, 3CL(pro) and endoribonuclease, NSP15 proteins of SARS-CoV-2. *Journal of Biomolecular Structure & Dynamics*, 40(1), 86–100. <https://doi.org/10.1080/07391102.2020.1808077>
- Skowronski, D. M., Astell, C., Brunham, R. C., Low, D. E., Petric, M., Roper, R. L., Talbot, P. J., Tam, T., & Babiuk, L. (2005). Severe acute respiratory syndrome (SARS): A year in review. *Annual Review of Medicine*, 56(1), 357–381. <https://doi.org/10.1146/annurev.med.56.091103.134135>

- Sousa da Silva, A. W., & Vranken, W. F. (2012). ACPYPE - AnteChamber PYthon Parser interfacE. *BMC Research Notes*, 5(1), 367. <https://doi.org/10.1186/1756-0500-5-367>
- Suan Li, M., & Khanh Mai, B. (2012). Steered molecular dynamics-a promising tool for drug design. *Current Bioinformatics*, 7(4), 342–351. <https://doi.org/10.2174/157489312803901009>
- Thai, N. Q., Linh, H. N., Linh, H. Q., & Li, M. S. (2017). Protocol for fast screening of multi-target drug candidates: Application to Alzheimer's disease. *Journal of Molecular Graphics & Modelling*, 77, 121–129. <https://doi.org/10.1016/j.jmgm.2017.08.002>
- Torrie, G. M., & Valleau, J. P. (1977). Nonphysical sampling distributions in Monte Carlo free-energy estimation: Umbrella sampling. *Journal of Computational Physics*, 23(2), 187–199. [https://doi.org/10.1016/0021-9991\(77\)90121-8](https://doi.org/10.1016/0021-9991(77)90121-8)
- Tripathi, P. K., Upadhyay, S., Singh, M., Raghavendhar, S., Bhardwaj, M., Sharma, P., & Patel, A. K. (2020). Screening and evaluation of approved drugs as inhibitors of main protease of SARS-CoV-2. *International Journal of Biological Macromolecules*, 164(1), 2622–2631. <https://doi.org/10.1016/j.ijbiomac.2020.08.166>
- Trott, O., & Olson, A. J. (2010). AutoDock Vina: improving the speed and accuracy of docking with a new scoring function, efficient optimization, and multithreading. *Journal of Computational Chemistry*, 31(2), 455–461. <https://doi.org/10.1002/jcc.21334>
- Viet, M.H., Siposova, K., Bednarikova, Z., Antosova, A., Nguyen, T. T., Gazova, Z., & Li, M. S. (2015). *In silico a n d in vitro* study of binding affinity of tripeptides to amyloid beta fibrils: Implications for Alzheimer's disease . *The Journal of Physical Chemistry B*, 119(16), 5145–5155. <https://doi.org/10.1021/acs.jpcc.5b00006>
- Viswanathan, T., Arya, S., Chan, S.-H., Qi, S., Dai, N., Misra, A., Park, J.-G., Oladunni, F., Kovalskyy, D., Hromas, R. A., Martinez-Sobrido, L., & Gupta, Y. K. (2020). Structural basis of RNA cap modification by SARS-CoV-2. *Nature Communications*, 11(1), 3718. <https://doi.org/10.1038/s41467-020-17496-8>
- Vuong, Q. V., Nguyen, T. T., & Li, M. S. (2015). A new method for navigating optimal direction for pulling ligand from binding pocket: Application to ranking binding affinity by steered molecular dynamics. *Journal of Chemical Information and Modeling*, 55(12), 2731–2738. <https://doi.org/10.1021/acs.jcim.5b00386>
- Wang, J., Wang, W., Kollman, P. A., & Case, D. A. (2001). Antechamber: An accessory software package for molecular mechanical calculations. *Journal of the American Chemical Society*, 222, U403.
- Wang, J., Wolf, R. M., Caldwell, J. W., Kollman, P. A., & Case, D. A. (2004). Development and testing of a general amber force field. *Journal of Computational Chemistry*, 25(9), 1157–1174. <https://doi.org/10.1002/jcc.20035>
- Wang, Y., Zhang, D., Du, G., Du, R., Zhao, J., Jin, Y., Fu, S., Gao, L., Cheng, Z., Lu, Q., Hu, Y., Luo, G., Wang, K., Lu, Y., Li, H., Wang, S., Ruan, S., Yang, C., Mei, C., ... Wang, C. (2020). Remdesivir in adults with severe COVID-19: A randomised, double-blind, placebo-controlled, multi-centre trial. *Lancet (London, England)*, 395(10236), 1569–1578. [https://doi.org/10.1016/S0140-6736\(20\)31022-9](https://doi.org/10.1016/S0140-6736(20)31022-9)
- White, M. A., Lin, W., & Cheng, X. (2020). Discovery of COVID-19 inhibitors targeting the SARS-CoV-2 Nsp13 helicase. *The Journal of Physical Chemistry Letters*, 11(21), 9144–9151. <https://doi.org/10.1021/acs.jpcclett.0c02421>
- WHO. (2021). Classification of omicron (B.1.1.529): SARS-CoV-2 variant of concern. [https://www.who.int/news/item/26-11-2021-classification-of-omicron-\(b.1.1.529\)-sars-cov-2-variant-of-concern](https://www.who.int/news/item/26-11-2021-classification-of-omicron-(b.1.1.529)-sars-cov-2-variant-of-concern)
- World Health Organization. (2020). *Coronavirus disease 2019 (COVID-19): Situation report* (Vol. 74). WHO.
- Yadav, R., Imran, M., Dhamija, P., Suchal, K., & Handu, S. (2021). Virtual screening and dynamics of potential inhibitors targeting RNA binding domain of nucleocapsid phosphoprotein from SARS-CoV-2. *Journal of Biomolecular Structure & Dynamics*, 39(12), 4433–4448. <https://doi.org/10.1080/07391102.2020.1778536>